$\nu\Lambda$CDM: Neutrinos help reconcile Planck with the Local Universe

Mark Wyman,* Douglas H. Rudd, R. Ali Vanderveld, and Wayne Hu
Kavli Institute for Cosmological Physics, Department of Astronomy & Astrophysics, Enrico Fermi Institute, University of Chicago, Chicago, Illinois 60637, U.S.A

Current measurements of the low and high redshift Universe are in tension if we restrict ourselves to the standard six parameter model of flat ΛCDM. This tension has two parts. First, the Planck satellite data suggest a higher normalization of matter perturbations than local measurements of galaxy clusters. Second, the expansion rate of the Universe today, H_0, derived from local distance-redshift measurements is significantly higher than that inferred using the acoustic scale in galaxy surveys and the Planck data as a standard ruler. The addition of a sterile neutrino species changes the acoustic scale and brings the two into agreement; meanwhile, adding mass to the active neutrinos or to a sterile neutrino can suppress the growth of structure, bringing the cluster data into better concordance as well. For our fiducial dataset combination, with statistical errors for clusters, a model with a massive sterile neutrino shows 3.5σ evidence for a non-zero mass and an even stronger rejection of the minimal model. A model with massive active neutrinos and a massless sterile neutrino is similarly preferred. An eV-scale sterile neutrino mass – of interest for short baseline and reactor anomalies – is well within the allowed range. We caution that 1) unknown astrophysical systematic errors in any of the data sets could weaken this conclusion, but they would need to be several times the known errors to eliminate the tensions entirely; 2) the results we find are at some variance with analyses that do not include cluster measurements; and 3) some tension remains among the datasets even when new neutrino physics is included.

arXiv:1307.7715v2 [astro-ph.CO] 2 Jan 2014

Neutrinos are one of the most elusive constituents of the standard model of particle physics. They interact only via the weak force and are nearly massless. In the standard picture, there are three neutrino species with a summed mass that solar and atmospheric oscillation observations bound to be above 0.06 eV (e.g. [1]). However, anomalies in short baseline and reactor neutrino experiments suggest that there may be one or more additional eV scale massive sterile neutrinos (see refs. [2, 3] for reviews).

Meanwhile, cosmological observations have established a standard model of cosmology – often called inflationary ΛCDM. With only six basic parameters, its most minimal incarnation can explain a wide range of phenomena, from light element abundances, through the cosmic microwave background (CMB) anisotropy and large scale structure, the formation and statistical properties of dark matter halos that host galaxy clusters to the current expansion history and cosmic acceleration. Precise new data allow us to test if the subtle effects of eV scale neutrinos and partially populated sterile species are also present.

Interestingly, the Planck satellite [4] has recently exposed potential tension between the early and late time observables in the minimal six parameter model. In particular, Planck finds a larger and more precisely measured matter density at recombination than previous data. This relatively small change at high redshift cascades into more dramatic implications for observables today (e.g. [5]): the current expansion rate, H_0, decreases and the amount of cosmological structure increases. These changes are in 2-3σ tension with direct observations of H_0 [6] and the abundance of galaxy clusters [7], respectively. Meanwhile, agreement with distance measures from baryon acoustic oscillations (BAO) [8–10] suggest that the former cannot be resolved by having evolving dark energy modify the recent expansion history.

Neutrinos offer a possible means of bringing these observations into concordance. Sterile neutrinos change the expansion rate at recombination and hence the calibration of the standard ruler with which CMB and BAO observations infer distances (e.g. [4]). When either the sterile or active species are massive, their free streaming reduces the amount of small scale clustering today and hence the tension with cluster measurements. In the simplest case, we can think of this modification as adding a single, massive sterile neutrino to the standard model.

Models and Data.– The minimal 6 parameter flat ΛCDM model is defined by $\{\Omega_c h^2, \Omega_b h^2, \tau, \theta_A, A_S, n_s\}$, where $\Omega_c h^2$ defines the cold dark matter (CDM) density, $\Omega_b h^2$ the baryon density, τ the Thomson optical depth to reionization, θ_A the angular acoustic scale at recombination, A_s the amplitude of the initial curvature power spectrum at $k = 0.05$ Mpc^{-1}, and n_s its spectral index. With precise constraints on these parameters from CMB data at high redshift, all other low redshift observables are precisely predicted: importantly the Hubble constant, $H_0 = 100h$ km/s/Mpc, the present total matter density Ω_m, and the rms amplitude of linear fluctuations today on the $8h^{-1}$Mpc scale, σ_8.

Conflict between these predictions and actual measurements may suggest a non-minimal model. In this context, we consider 3 new neutrino parameters: $N_{\rm eff}$, $\sum m_\nu$, and m_s. We define $N_{\rm eff}$, the effective number of relativistic species, via the relativistic energy density at high redshift

$$\rho_{\rm r} = \rho_\gamma + \rho_\nu = \left[1 + \frac{7}{8}\left(\frac{4}{11}\right)^{4/3} N_{\rm eff}\right]\rho_\gamma. \qquad (1)$$

TABLE I. Models and data combinations studied.

Model	ΛCDM (6)	$N_{\rm eff}$	$\sum m_\nu$	m_s
M(inimal)ν	✓	3.046	0.06eV	0
S(terile)ν	✓	✓	0.06eV	✓
A(ctive)ν	✓	✓	✓	0

Data	M(inimal)d	T(ension)d	A(ll)d
Planck [4] +WMAP P. [11]	✓	✓	✓
H_0 [6]		✓	✓
BAO [8–10]		✓	✓
X-ray Clusters [7]		✓	✓
SNe (Union2) [12]			✓
High-ℓ CMB [13–15]			✓

In the minimal model $N_{\rm eff} = 3.046$. Any value of $N_{\rm eff}$ larger than this fiducial value corresponds to a greater expansion rate in the early Universe, consistent with the presence of some extra density of relativistic particles, which includes neutrinos beyond the 3 known "active" species. Next, $\sum m_\nu$ denotes the summed mass of the active neutrinos. It is at least 0.06 eV, from mass squared splittings in solar and atmospheric oscillations, but in principle could be larger if the species are nearly degenerate in mass. We call the model with $N_{\rm eff} = 3.046$, $\sum m_\nu = 0.06$eV the "minimal neutrino" (Mν) mass model.

Finally, we introduce an effective mass m_s for the 4th, mostly sterile, species by requiring that the total neutrino contribution to the energy density today is given by

$$(94.1\,{\rm eV})\Omega_\nu h^2 = (3.046/3)^{3/4}\sum m_\nu + m_s. \qquad (2)$$

We do not study all three extra parameters simultaneously, but instead vary $N_{\rm eff}$ together with either $\sum m_\nu$ or m_s – see Table I. When we allow m_s to vary we set $\sum m_\nu = 0.06$eV and call it the "sterile neutrino" (Sν) mass model. Similarly, we explore an "active neutrino" (Aν) model, allowing $\sum m_\nu$ to vary with the masses assumed to be degenerate and setting $m_s = 0$. We define the total non-relativistic matter density today as $\Omega_m = \Omega_c + \Omega_b + \Omega_\nu$.

Note that m_s is not the true mass of a new neutrino-like particle, but rather encapsulates both the particle's mass and how this species was populated in the early universe. This effective mass is typically related to the true mass in one of two ways. If the extra sterile neutrino species are thermally distributed, we have $m_s^{\rm T} = (\Delta N_{\rm eff})^{-3/4} m_s$, where we have defined $\Delta N_{\rm eff} = N_{\rm eff} - 3.046 \equiv (T_\nu/T_s)^3$. Alternatively, if the new sterile neutrino(s) are distributed proportionally to the active neutrinos due to oscillations, we have, following Dodelson and Widrow [16], $m_s^{\rm DW} = (\Delta N_{\rm eff})^{-1} m_s$. Since the effective parameter that enters the cosmological analysis is the same in both cases, the choice only impacts the interpretation and external priors. For the latter, we take a $m_s^{\rm DW} < 7$eV prior to prevent trading very massive neutrinos with CDM – a degeneracy which is not of interest for eV scale neutrino physics. Note that we use this condition to set an allowed prior range in the m_s-$\Delta N_{\rm eff}$ plane. We will otherwise take flat priors on the separate m_s and $\Delta N_{\rm eff}$ parameters.

To explore constraints on these parameters given the various cosmological data sets, we sample their posterior probability with the Monte Carlo Markov Chain technique using the CosmoMC code [17] for the various data sets summarized in Table I. Common to all sets is the CMB temperature data from the Planck satellite [4] together with polarization data from the WMAP satellite [11], dubbed the "minimal" dataset (Md). Here we marginalize the standard foreground nuisance parameters provided by Planck. Note that CosmoMC in practice uses an approximation to the acoustic scale $\theta_{\rm MC} \approx \theta_A$ and uses $\ln A = \ln(10^{10} A_S)$.

Next, we add datasets that reveal the presence of tension with the Mν model. These are the H_0 inference from the maser-cepheid-supernovae distance ladder [6], BAO measurements [8–10] and the X-ray cluster abundance [18] [19]. We call this combined dataset the "tension" dataset (Td). This is the minimal set of data required to expose tension. The BAO data, which also measure the low redshift distance-redshift relation, prevent explaining H_0 with smooth changes in the expansion history toward phantom equations of state [4]. Thus, we include the BAO data in the "tension" dataset because it confirms the existence of tension, not because it is itself in tension with Planck. Conversely, clusters alone might be explained by exotic dark energy that reduces the linear growth rate; but when combined with these distance measurements, the data point to neutrinos instead.

For the cluster data, we also separately test a systematic 9% increase in the mass calibration of local clusters [7] to show the shift in some of our statistics. Use of such a shift was proposed by the authors of [7]; its size was based on a variety of X-ray, optical, Sunyaev-Zel'dovich, and lensing mass observables (see e.g. [20]). Finally, we add the Union2 compilation of type Ia supernovae [12] and high resolution CMB data [21] from the ACT [15] and SPT [13, 14] telescopes in the "all" dataset (Ad).

Results.– We start with the basic minimal neutrino model and minimal Planck-WMAP dataset case (Mν-Md) shown in Tab. II (column 1). From the fundamental chain parameters, we can derive the posterior probability distributions for two auxiliary parameters, H_0 and $S_8 = \sigma_8(\Omega_m/0.25)^{0.47}$ – see Fig. 1. The latter effectively controls the local cluster abundance. Very little overlap exists between the Mν-Md predictions for these local observables and the measurements (68% confidence bands). Even adding a 9% systematic shift in the cluster masses

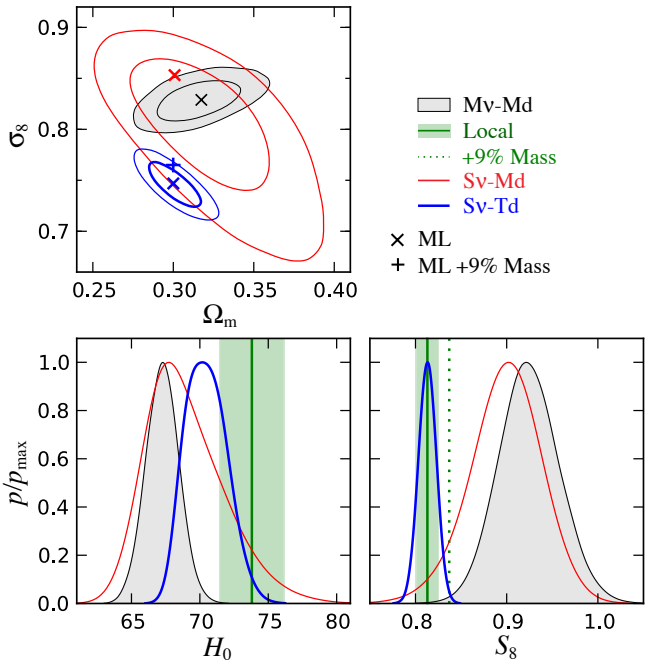


FIG. 1. Tensions between datasets and their neutrino alleviations. Black, red, and blue curves represent the Mν-Md, Sν-Md, and Sν-Td model-data combinations respectively. *Bottom:* H_0 and S_8 posteriors (curves) vs. local measurements (bands, 68% CL). Lack of overlap in Mν-Md is alleviated in Sν-Md leading to better concordance in Sν-Td. The dashed line shows the change in S_8 from the 9% cluster mass offset. *Top:* σ_8 and Ω_m 68% and 95% confidence regions. Neutrino parameters open a direction mainly orthogonal to S_8. "×" marks ML models; "+" shows its shift for a 9% cluster mass offset. Aν model results are similar.

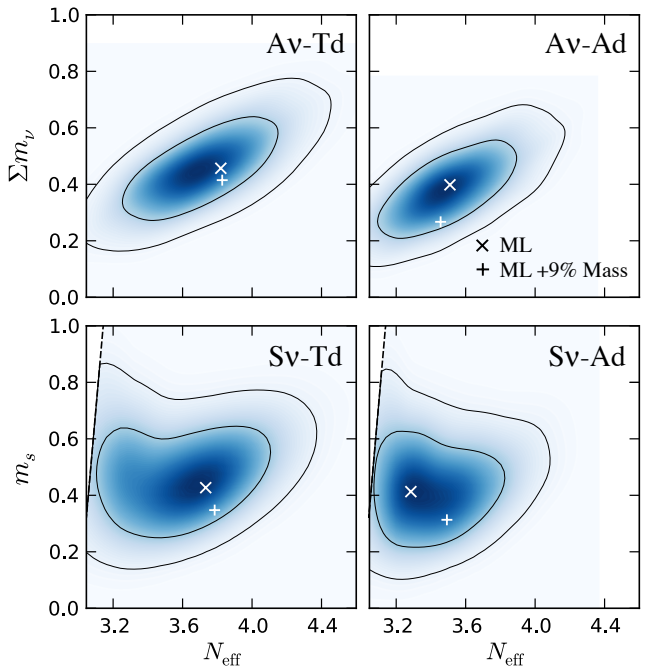


FIG. 2. Neutrino mass and effective number constraints, labelled as in Fig. 1 (× indicates the ML model, + its shift from a 9% cluster mass increase). *Bottom:* Sν sterile case for Td (left) and Ad (right). The region excluded by the $m_s^{\rm DW} < 7$eV prior is left of the dashed line. *Top:* Aν active case for Td (left) and Ad (right). In all cases the minimal $\sum m_\nu = 0.06$eV, $N_{\rm eff} = 3.046$ and $m_s = 0$ is highly excluded.

is insufficient to bring about concordance.

These predictions depend on our assumptions about neutrinos. The presence of extra relativistic species in the early Universe alters the expansion rate and thus the physical length scale associated with both the CMB and the BAO. Allowing $N_{\rm eff}$ to vary changes this scale and broadens the allowed range for H_0. In Fig. 1 (bottom), we see that in the Sν case, the H_0 posterior implied by Md broadens to include substantial overlap with the measurements. A similar broadening occurs for the Aν case.

Allowing part of the matter to be composed of neutrinos with eV scale masses suppresses the growth of structure below their free-streaming length. This allows σ_8 to be substantially lower and still be compatible with the Md CMB datasets (see Fig. 1). However, since the CDM component $\Omega_c h^2$ is well constrained independently, adding neutrinos increases Ω_m, leading to a less pronounced modification to the cluster observable (see Fig. 1, bottom right and top panels). Also, raising $N_{\rm eff}$ to reduce the H_0 tension requires an increase in the tilt n_s to compensate for the reduction of power in the CMB damping tail, which further reduces the impact (see e.g. [22] Fig. 3). Nonetheless the overlap between the posterior of the Md dataset and the measurements is now visible for the Sν model, whereas it was negligible with the Mν model. Furthermore, a 9% shift in cluster masses now brings the observations into reasonable concordance. Slightly more tension remains in the Aν case because spreading the mass among three species gives lower true masses for each. Including the BAO and H_0 data also somewhat enhance the residual tension with high mass [23].

A joint analysis of the Td data set supports these conclusions (see Tab. II). For the Sν model, the minimal neutrino values of $m_s = 0$ and $N_{\rm eff} = 3.046$ are individually disfavored at 3.5σ and 2σ respectively. Fig. 2 shows that the joint exclusion is even stronger, with the minimal $N_{\rm eff}$ at $m_s = 0$ rejected at high confidence. The maximum likelihood (ML) Sν model has a $2\Delta \ln \mathcal{L} = 15.5$ with two extra parameters ($m_s = 0.43$eV and $N_{\rm eff} = 3.73$) over that of the Mν model. Note that these two parameters combine to imply an actual ML mass $m_s^{\rm DW} = 0.62$eV. For the Aν-Td case, the minimal $\sum m_\nu$ and $N_{\rm eff}$ are disfavored at 3.4σ and 2.3σ respectively with $2\Delta \ln \mathcal{L} = 14.05$ ($\sum m_\nu = 0.46$eV, $N_{\rm eff} = 3.82$).

Including all of the data with Ad reduces these preferences somewhat (see Tab. II and Fig. 2). This is mainly due to the high resolution CMB data which can break degeneracies between parameters like $N_{\rm eff}$ and n_s. But the preference for non-minimal masses remains: 3.2σ and

TABLE II. Summary of posterior statistics. Ω_m, H_0 and S_8 are derived parameters and $2\Delta\ln\mathcal{L}$ gives the likelihood of the ML model of the non-minimal neutrino model relative to the minimal Mν model with the same dataset. Upper limits are 68% CL.

Data	Md			Td		Ad	
Model	Mν	Sν	Aν	Sν	Aν	Sν	Aν
$2\Delta\ln\mathcal{L}$	–	0.5	0.9	15.5	14.1	11.9	9.7
$100\Omega_b h^2$	2.204 ± 0.028	2.236 ± 0.036	2.222 ± 0.046	2.272 ± 0.027	2.275 ± 0.028	2.272 ± 0.027	2.273 ± 0.028
$\Omega_c h^2$	0.1199 ± 0.0027	0.1263 ± 0.0052	0.1255 ± 0.0053	0.1210 ± 0.0050	0.1229 ± 0.0044	0.1183 ± 0.0040	0.1196 ± 0.0038
$100\theta_{\rm MC}$	1.0413 ± 0.0006	1.0406 ± 0.0007	1.0407 ± 0.0008	1.0412 ± 0.0007	1.0409 ± 0.0007	1.0414 ± 0.0006	1.0413 ± 0.0007
τ	0.090 ± 0.013	0.095 ± 0.015	0.094 ± 0.014	0.096 ± 0.015	0.096 ± 0.015	0.096 ± 0.014	0.096 ± 0.015
n_s	0.9604 ± 0.0072	0.9748 ± 0.0148	0.9721 ± 0.0175	0.9857 ± 0.0120	0.9939 ± 0.0097	0.9798 ± 0.0108	0.9877 ± 0.0096
$\ln A$	3.089 ± 0.025	3.116 ± 0.031	3.110 ± 0.033	3.107 ± 0.031	3.109 ± 0.031	3.101 ± 0.030	3.100 ± 0.032
$N_{\rm eff}$	–	3.56 ± 0.31	3.44 ± 0.38	3.61 ± 0.31	3.72 ± 0.29	3.44 ± 0.23	3.51 ± 0.26
Σm_ν,m_s	–	< 0.34	< 0.32	0.48 ± 0.14	0.46 ± 0.12	0.44 ± 0.14	0.39 ± 0.11
Ω_m	0.316 ± 0.017	0.322 ± 0.028	0.331 ± 0.050	0.301 ± 0.010	0.299 ± 0.011	0.298 ± 0.010	0.296 ± 0.010
H_0	67.3 ± 1.2	69.0 ± 2.8	67.9 ± 4.5	70.5 ± 1.5	70.9 ± 1.4	70.0 ± 1.2	70.4 ± 1.4
S_8	0.925 ± 0.033	0.899 ± 0.038	0.908 ± 0.036	0.813 ± 0.010	0.815 ± 0.009	0.813 ± 0.010	0.815 ± 0.009

3σ evidence (with improvements of $2\Delta\ln\mathcal{L} = 11.9$ and 9.7) for the Sν and Aν cases respectively.

With a 9% cluster mass offset, lower neutrino masses are preferred. For example, in the Sν-Td case the ML model shifts from $m_s = 0.43$eV to 0.35eV with ML improvement of Sν over Mν of $2\Delta\ln\mathcal{L} = 9.6$. For the A$\nu$-Td case it shifts from $\sum m_\nu = 0.46$eV to 0.41eV with $2\Delta\ln\mathcal{L} = 8.4$. Other cases are shown in Fig. 2 and all are within the 68% joint CL regions.

Discussion.– Taken at face-value, these results indicate $\sim 3\sigma$ statistical evidence for non-minimal neutrino parameters, especially in their masses, which simultaneously brings concordance in the CMB, BAO, H_0, and cluster data. The addition of other datasets, such as supernovae or high-ℓ CMB measurements, refine but do not qualitatively change this conclusion.

Conversely, unknown systematic errors in any of the Td data sets could alter our conclusions substantially. For Planck these include the modeling of foregrounds and instrumental effects, especially at high multipole, and for H_0 the calibration of the supernova distance ladder. The preference for high neutrino mass(es) is mainly driven by the cluster data set (cf. Ref. [23] who find upper limits without clusters). As such, the best fitting parameter values we find are in mild tension with results from combinations of datasets that exclude clusters. However, the improvement in the agreement with the cluster data is sufficiently strong to more than compensate, in a likelihood maximization sense, for this slight worsening of the fit to the other data. In light of these various concerns – especially the remaining tension even with new neutrino physics included – a more thoroughgoing model-selection analysis of these data will certainly be warranted in the future, especially as the systematic errors in each of the datasets become better quantified. Regardless, if future data or analyses lead to increased mass estimates for the clusters, that change would weaken the preference we find. However, the preference can only be eliminated if the systematic shift is roughly triple the 9% estimate. As mention before, this cluster mass calibration error estimate comes from comparing a variety of X-ray, optical, Sunyaev-Zel'dovich, and lensing observables (see e.g. [20] for a recent assessment). We also note that the Planck Sunyaev-Zeldovich cluster results are consistent with the dataset we have used, and their analysis of neutrino physics agrees with ours where the two overlap; however, the Planck collaboration did not directly test the neutrino models that we have used in their analyses [24].

Other cosmological data sets can also cross check these conclusions. Indeed, there is mild tension with the shape of galaxy power spectra [25, 26] but these come with their own astrophysical systematics in the interpretation of galaxy bias, and those systematics are more difficult to address than those affecting cluster mass estimates. In the future, weak lensing of the CMB and galaxies should definitively test this result.

Acknowledgments.– We thank E. Rozo, A. Zablocki, and S. Dodelson for helpful discussions. This work was supported at the KICP through grants NSF PHY-0114422 and NSF PHY-0551142 and an endowment from the Kavli Foundation. MW and WH were additionally supported by U.S. Dept. of Energy contract DE-FG02-90ER-40560. This work made use of computing resources provided by the Research Computing Center at the University of Chicago.

* markwy@oddjob.uchicago.edu

[1] M. Gonzalez-Garcia, M. Maltoni, J. Salvado, and T. Schwetz, JHEP **1212**, 123 (2012), arXiv:1209.3023 [hep-ph].

[2] J. M. Conrad, W. C. Louis, and M. H. Shaevitz, Ann.Rev.Nucl.Part.Sci. **63**, 45 (2013), arXiv:1306.6494 [hep-ex].

[3] K. Abazajian, M. Acero, S. Agarwalla, A. Aguilar-Arevalo, C. Albright, *et al.*, (2012), arXiv:1204.5379 [hep-ph].

[4] P. Ade *et al.* (Planck Collaboration), (2013), arXiv:1303.5076 [astro-ph.CO].

[5] W. Hu, ASP Conf.Ser. **339**, 215 (2005), arXiv:astro-ph/0407158 [astro-ph].

[6] A. G. Riess, L. Macri, S. Casertano, H. Lampeitl, H. C. Ferguson, *et al.*, Astrophys.J. **730**, 119 (2011), arXiv:1103.2976 [astro-ph.CO].

[7] A. Vikhlinin, A. Kravtsov, R. Burenin, H. Ebeling, W. Forman, *et al.*, Astrophys.J. **692**, 1060 (2009), arXiv:0812.2720 [astro-ph].

[8] L. Anderson, E. Aubourg, S. Bailey, D. Bizyaev, M. Blanton, *et al.*, Mon.Not.Roy.Astron.Soc. **428**, 1036 (2013), arXiv:1203.6594 [astro-ph.CO].

[9] N. Padmanabhan, X. Xu, D. J. Eisenstein, R. Scalzo, A. J. Cuesta, *et al.*, Mon.Not.Roy.Astron.Soc. **427**, 2132 (2012), arXiv:1202.0090 [astro-ph.CO].

[10] C. Blake, E. Kazin, F. Beutler, T. Davis, D. Parkinson, *et al.*, Mon.Not.Roy.Astron.Soc. **418**, 1707 (2011), arXiv:1108.2635 [astro-ph.CO].

[11] C. Bennett, D. Larson, J. Weiland, N. Jarosik, G. Hinshaw, *et al.*, (2012), arXiv:1212.5225 [astro-ph.CO].

[12] N. Suzuki, D. Rubin, C. Lidman, G. Aldering, R. Amanullah, *et al.*, Astrophys.J. **746**, 85 (2012), arXiv:1105.3470 [astro-ph.CO].

[13] C. Reichardt, L. Shaw, O. Zahn, K. Aird, B. Benson, *et al.*, Astrophys.J. **755**, 70 (2012), arXiv:1111.0932 [astro-ph.CO].

[14] R. Keisler, C. Reichardt, K. Aird, B. Benson, L. Bleem, *et al.*, Astrophys.J. **743**, 28 (2011), arXiv:1105.3182 [astro-ph.CO].

[15] S. Das, T. Louis, M. R. Nolta, G. E. Addison, E. S. Battistelli, *et al.*, (2013), arXiv:1301.1037 [astro-ph.CO].

[16] S. Dodelson and L. M. Widrow, Phys.Rev.Lett. **72**, 17 (1994), arXiv:hep-ph/9303287 [hep-ph].

[17] A. Lewis and S. Bridle, Phys. Rev. **D66**, 103511 (2002), astro-ph/0205436.

[18] R. A. Burenin and A. A. Vikhlinin, Astronomy Letters **38**, 347 (2012), arXiv:1202.2889 [astro-ph.CO].

[19] The cluster abundance is included in the likelihood analysis via the likelihood code released simultaneously with [18].

[20] E. Rozo, E. S. Rykoff, J. G. Bartlett, and A. E. Evrard, (2013), arXiv:1302.5086 [astro-ph.CO].

[21] J. Dunkley, E. Calabrese, J. Sievers, G. Addison, N. Battaglia, *et al.*, (2013), arXiv:1301.0776 [astro-ph.CO].

[22] R. A. Vanderveld and W. Hu, Phys.Rev. **D87**, 063510 (2013), arXiv:1212.3608 [astro-ph.CO].

[23] L. Verde, S. M. Feeney, D. J. Mortlock, and H. V. Peiris, (2013), arXiv:1307.2904 [astro-ph.CO].

[24] P. Ade *et al.* (Planck Collaboration), (2013), arXiv:1303.5080 [astro-ph.CO].

[25] S. Riemer-Sorensen, D. Parkinson, and T. M. Davis, (2013), arXiv:1306.4153 [astro-ph.CO].

[26] E. Giusarma, R. de Putter, S. Ho, and O. Mena, (2013), arXiv:1306.5544 [astro-ph.CO].